

# Electromagnetic wave absorption potential of SiC-based ceramic woven fabrics in the GHz range

E. Tan · Y. Kagawa · A. F. Dericioglu

Received: 20 May 2008 / Accepted: 8 January 2009 / Published online: 4 February 2009  
© Springer Science+Business Media, LLC 2009

**Abstract** This article investigates the electromagnetic wave-absorbing properties of SiC-based ceramic woven fabrics. The electrical conductivity of ceramic woven fabrics was modified by heat treatment in air, resulting in oxidation, and the electromagnetic wave absorption potential of single- and double-layer ceramic woven fabrics were determined in the 17–40 GHz frequency range using the free-space method. The absorption potentials of ceramic woven fabrics of different chemical composition and weave were correlated with their material properties through X-ray diffraction, scanning electron microscopy, and electrical resistance measurement. The effect of the different arrangements of fabrics in multilayer forms, and how oxidation affects the electromagnetic wave absorption potential of the fabrics are discussed. Various double-layer combinations of SiC-based woven fabrics revealed promising potentials for both reduced reflection and transmission, resulting in ~90% absorption in the GHz range, which makes them powerful candidate materials for electromagnetic wave absorption applications.

## Introduction

The rapid development of advanced electronic devices and applications has brought with it a growing interest in electromagnetic wave-absorbing materials. Many commercial and military applications, such as data transmission, telecommunications, wireless network systems, and satellite broadcasting, as well as radars, and diagnostic and detection systems, utilize and emit electromagnetic waves. The interaction of electromagnetic waves originating from different sources can lead to a decrease in quality and a misinterpretation of transferred data, and it has thus become vital to avoid such interference and electromagnetic wave pollution through the use of appropriate absorbing and shielding materials.

Electromagnetic wave-absorbing materials absorb and dissipate electromagnetic energy to which they are exposed, reducing reflected and/or scattered electromagnetic components to a minimum [1]. There are various magnetic lossy materials, such as ferrites, carbonyl iron, cobalt, and so on, which when dispersed in polymers can be used as magnetic absorbers [2–5]. The main drawbacks of these materials are that they are heavy, and are only effective only in the MHz range [6, 7]. On the other hand, lossy dielectric materials stand out due to their low density and effectiveness in the GHz frequency range. Composites with conductive powders, such as carbon black and graphite [6, 8, 9], as well as continuous or discontinuous conducting fillers [10–12], are used as dielectric absorbers, generating dielectric loss by improving the electrical conductivity of the mixture.

In this study, the electromagnetic wave-absorbing potentials of dielectric lossy materials, in this case SiC-based ceramic woven fabrics, were investigated. These fabrics are typically used as reinforcement for high-temperature

---

E. Tan · A. F. Dericioglu (✉)  
Department of Metallurgical and Materials Engineering, Middle East Technical University, Inonu Bulv., 06531 Ankara, Turkey  
e-mail: arcan@metu.edu.tr

Y. Kagawa  
Research Center for Advanced Science and Technology,  
The University of Tokyo, 4-6-1 Komaba, Meguro-ku,  
Tokyo 153-8904, Japan

structural ceramic composites due to their strength and stability at high temperatures [13–15]. Despite the intrinsic properties of these woven fabrics, such as their high specific modulus and strength, low density and environmental durability related to their structural use, little is known about their interaction with electromagnetic radiation in the GHz range [16, 17], although they have a wide range of electrical resistance, from  $10^{-3}$  to  $10^4 \Omega\text{m}$  [18]. The desired property set of low weight, high environmental durability, low thickness, and wide electrical resistance range makes these materials attractive for electromagnetic wave-absorbing applications; and consequently this study focuses on the characteristics of the interaction between SiC-based ceramic woven fabrics and electromagnetic waves. The electrical conductivities of ceramic woven fabrics were modified by heat treatment in air, and the electromagnetic wave absorption potential of single and various double-layer combinations of ceramic woven fabrics were determined in the 17–40 GHz frequency range using the “free-space” method. The effects of alternating woven fabrics in multi-layer form and oxidation on the resulting interaction with electromagnetic waves were discussed.

### Experimental procedure

#### Materials and heat treatment

The materials selected for this study were three SiC-based satin and plain woven fabrics (Tyranno<sup>®</sup>, Ube Industries, Co., Ltd, Ube, Yamaguchi, Japan) of different chemical compositions. Table 1 lists the basic properties of three different types of woven fabrics (S8, ZE8, and PN), as provided by the manufacturer [18]. The S8 and PN fabrics can be seen to have similar chemical compositions (Si, Ti, and C content), the exception being that PN fabric possesses a carbon-rich layer on its surface. The ZE8 fabric, on the other hand, has a higher carbon and silicon content than the other two, and contains zirconium in place of the titanium found in the PN and S8 fabrics. There are also variations between the fabrics in terms of the weave, with

the S8 and ZE8 fabrics being of a satin weave, while the PN fabric is plain woven.

The three materials were tested both in their as-received state and following heat treatment. The as-received ceramic woven fabrics were kept in air at 1573 K for 3 h to investigate the effect of heat treatment on their electromagnetic wave absorption properties.

#### Characterization of materials properties

The crystal structures of the as-received and heat-treated SiC-based ceramic woven fabrics were examined using X-ray diffraction (XRD), performed on an X-ray diffractometer (RINT 2200, Rigaku Corporation, Tokyo, Japan) with Cu  $K_\alpha$  radiation in the  $2\theta$  range from 20 to  $90^\circ$  with steps of  $0.02^\circ$ . A microstructural analysis was carried out using a scanning electron microscope (SEM) (JSM-6400, Jeol Ltd, Tokyo).

Bundles of fibers from each of the materials (shown in Table 1) were tested for electrical resistance using a DC voltage source, using silver paste in order to ensure a good electrical contact. A constant voltage was applied through the bundle, and the magnitude of the current was recorded for different voltage values. The average resistance,  $R$ , was determined using Ohm’s law, and the resistivity of each bundle,  $\rho$ , was calculated using Eq. 1, where  $l$  and  $A$  are the length and cross-sectional area of the bundle, respectively. The electrical conductivities,  $\sigma$ , of the as-received and heat-treated woven fabrics were determined by taking a reciprocal of their resistivity.

$$R = \rho \frac{l}{A} \tag{1}$$

#### Electromagnetic transmission and reflection measurements using the free-space method

The electromagnetic wave absorption potential of materials has been evaluated either directly through the measurement of reflectance and transmittance of electromagnetic waves using appropriate electronic systems or indirectly through the observation of changes in various physical properties including conductivity, dielectric constant, and temperature [19]. In this study, the reflection loss and transmission loss of the ceramic woven fabrics were directly determined in the 17–40 GHz frequency range using the free-space method. This measurement technique was preferred over the conventional contact method, as measurement accuracy is not so strongly dependent on the precision of the machining of the samples. In addition, an accurate measurement of the electromagnetic properties of anisotropic and inhomogeneous media, such as ceramics and composites, can be performed using the free-space method

**Table 1** Properties of fibers used in this study

Code of Tyranno <sup>®</sup> woven fabric	S8	ZE8	PN (C-coated)
Chemical composition (wt%)	Si: 50, C: 30 O: 18, Ti: 2	Si: 59, C: 38 O: 2, Zr: 1	Si: 50, C: 30 O: 18, Ti: 2
Weave type	Satin	Satin	Plain
Fiber diameter ( $\mu\text{m}$ )	8.5	13	8.5
Number of fibers per bundle	1600	400	1600
Density ( $\text{g}/\text{cm}^3$ )	2.35	2.55	2.39

without the excitation of higher-order modes, which is seldom possible with conventional methods. Furthermore, during the application of the free-space method the measurement is carried out in a non-destructive manner and without contact [20].

The free-space measurement system used in this study is schematically illustrated in Fig. 1. The equipment used for the measurement comprises a pair of spot-focusing type horn antennas (transmitting and receiving), a sample holder, and a coaxial cable connected to a HP8722D network analyzer. The horn antennas were equipped with biconvex polymeric lenses, focusing the electromagnetic waves on to the sample with a spot diameter  $\sim 2$ – $3$  times that of the wave under consideration. The antennas were separated by a distance measuring twice the focal length (330 mm) of the lenses. The horn antenna (I) sends an electromagnetic wave onto the surface of the sample; and the waves transmitted through and reflected from the sample were collected by horn antennas (II) and (I), respectively.

In order to minimize the measurement inaccuracies in the system, a through-reflect-line (TRL) calibration was carried out, whereas a time-domain gating was used to minimize the effects of residual mismatches, such as a mismatch in the source and load impedance [21]. After calibration, the woven fabrics were attached to a square cross-sectioned cardboard frame, and were placed into the sample holder mid-way between two spot-focusing horn lens antennas. The reflected and transmitted portions of the electromagnetic wave were determined for single-layer woven fabrics in the frequency range of the spot-focusing horn lens antennas (17–40 GHz). Measurements were also carried out on various double-layer combinations of fabrics, in both in their as-received state and after heat treatment to determine the effect of changing the electrical conductivity and sequencing of layers on electromagnetic wave absorption potential. These combinations were measured by arranging two cardboard frame sets with sample fabrics back-to-back in the

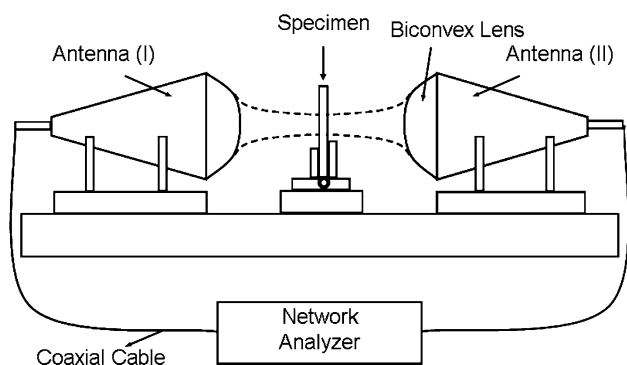


**Fig. 1** Schematic of the free-space measurement system used in the study

sample holder. In this way, double-layer combinations with a 1-mm spacing (thickness of the cardboard) between the layers were obtained, and the electromagnetic wave reflection and transmission losses of all combinations were examined through a repetition of the above procedure.

## Results and discussion

### General characteristics of SiC-based woven fabrics

The typical XRD patterns of the as-received and heat-treated SiC-based ceramic woven fabrics are shown in Fig. 2. The peaks show some broadening due to the small grain size of the fibers. The existence of three peaks in the  $2\theta$  values of 35.9, 60.2, and 71.8° showed the presence of  $\beta$ -SiC, detected in both the as-received and heat-treated samples. However, after the heat treatment an additional phase, SiO<sub>2</sub> ( $\alpha$ -cristobalite), was identified at around the  $2\theta$  value of 22.0°, indicating oxidation of the sample. This passive oxidation leads to the formation of a protective silica film, protecting the fibers from further oxidation [22]. Under equilibrium conditions, quartz is the stable phase at room temperature; however, in this case cooling from 1573 K (heat-treatment temperature) was not slow enough for reconstructive phase transitions from cristobalite to quartz, which resulted in a displacive transition, causing the distortion of cristobalite and the existence of  $\alpha$ -cristobalite at room temperature [23].

Figure 3a shows the SEM micrographs of the as-received PN-type fibers. A continuous oxide layer can be observed on the surface of the fibers on the SEM micrograph of the heat-treated PN (PN-H) fabric (Fig. 3b). In some areas the continuity of the oxide layer was lost,

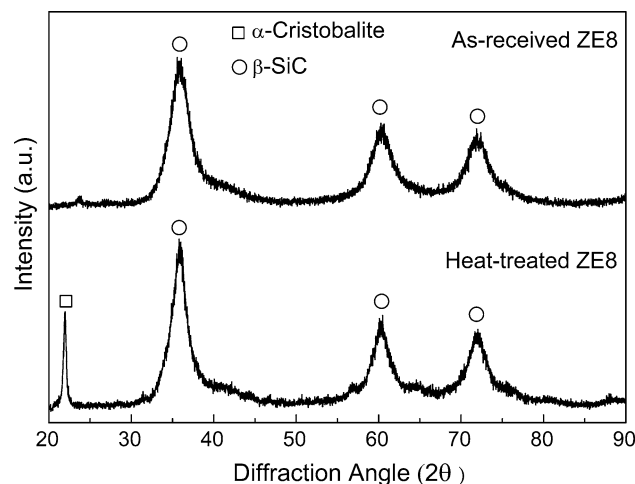


**Fig. 2** Typical XRD spectra of as-received and heat-treated SiC-based ceramic woven fabrics

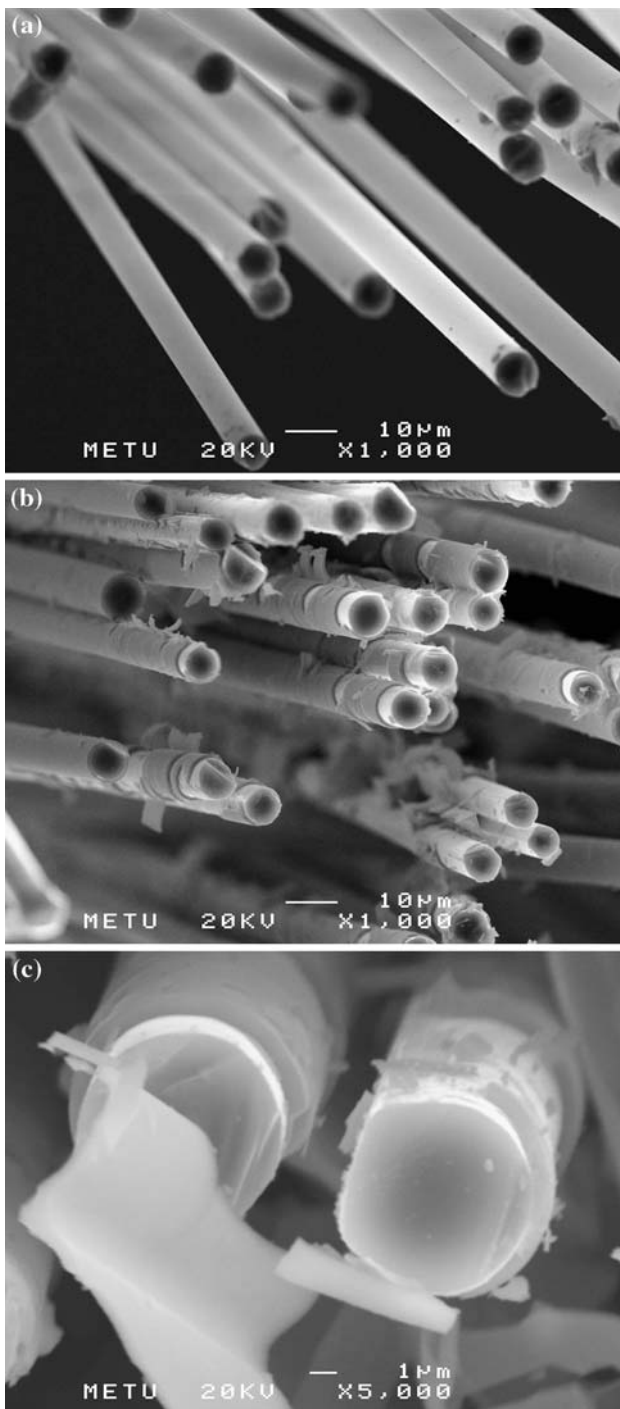


**Fig. 3** SEM micrographs of (a) as-received PN- and (b, c) PN-H-type woven fabrics at two different magnifications

most probably during handling of the bundles in the course of the observation of the fracture surface. At a higher magnification, the thickness of the oxide layer around the fiber was determined to be  $\sim 1 \mu\text{m}$  (Fig. 3c). The morphology and structure of the S8-type fibers showed similar characteristics to the PN-type in both as-received and heat-treated states.

Micrographs of the as-received and heat-treated ZE8 (ZE8-H)-type fibers are shown in Fig. 4a and b, respectively. In the case of the ZE8-H, detailed observations revealed that there was no clear continuous oxide layer around the fibers, but rather only localized oxidation of the fiber, indicated by arrows in Fig. 4b. The ZE8 fabric is described as heat resistant by the manufacturer, a claim that is verified by the results of our experiments.

Table 2 shows the electrical conductivity measurement results of the as-received and heat-treated SiC-based

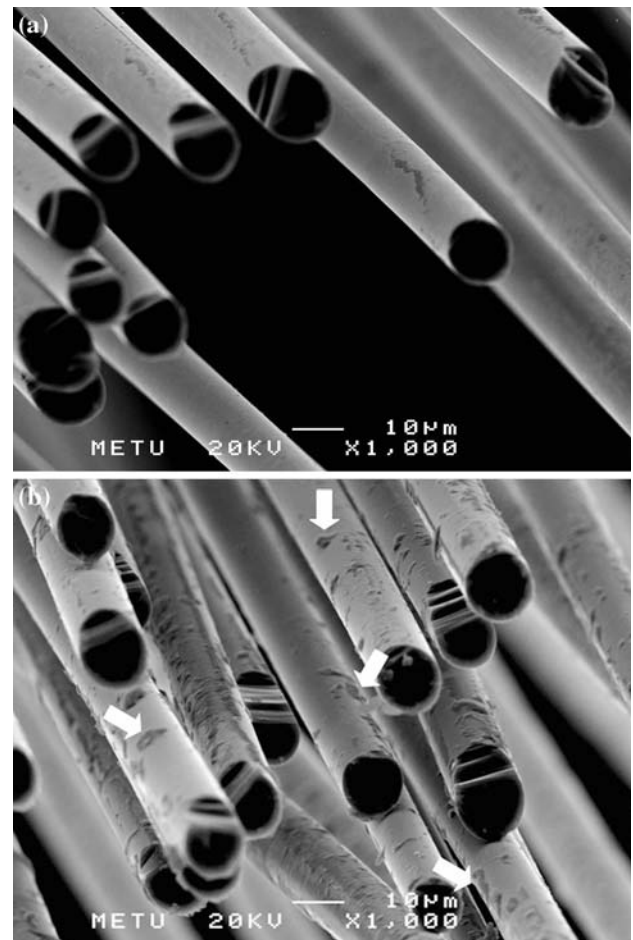


**Fig. 4** SEM micrographs of (a) as-received ZE8- and (b) ZE8-H-type woven fabrics

**Table 2** Electrical conductivity measurement results of used fibers

Fiber condition	Fiber type	DC conductivity (S/m)
As-received	S8	33.6
	ZE8	226.5
	PN	131.8
Heat-treated	S8	2.8
	ZE8	25.8
	PN	0.1



ceramic fibers. The as-received ZE8 fiber had the highest electrical conductivity among the samples, which can be explained by its higher Si and C content when compared with the other two fibers. After heat treatment, the ZE8 fiber maintained this tendency, acquiring the highest conductivity value among the heat-treated fibers. The results of the electrical conductivity measurements of the as-received and heat-treated SiC-based ceramic fibers showed that electrical conductivity decreases significantly following heat treatment, accounted for by the formation of an oxide layer around the fibers. The lack of an explicit continuous oxide layer could have resulted in the lower electrical conductivity decrease in the ZE8-type fiber.

#### Interaction of ceramic woven fabrics with electromagnetic radiation

The parameters used to quantify the interaction of electromagnetic waves with the woven fabrics—reflection loss,  $R_{\text{dB}}$ , and transmission loss,  $T_{\text{dB}}$ —were measured in the 17–40 GHz frequency range using the free-space method. The fractions of reflected and transmitted waves were calculated using Eq. 2, where  $P_0$ ,  $P_R$ ,  $P_T$  show the incident, reflected, and transmitted wave powers, respectively.

$$R_{\text{dB}} = 10 \log \left| \frac{P_R}{P_0} \right|; \quad T_{\text{dB}} = 10 \log \left| \frac{P_T}{P_0} \right|. \quad (2)$$

The changes in reflection loss in the as-received and heat-treated SiC-based ceramic woven fabrics are presented in Fig. 5a and b, respectively, measured in decibels (dB) as a function of frequency. A decrease in reflection loss (increasing negative dB) indicates that the reflected portion of the electromagnetic wave from the material surface is diminished. The ZE8 fabric recorded the highest reflection loss among all the as-received fabrics in the 17–40 GHz frequency range (Fig. 5a). Electrical conductivity has a marked effect on the reflection loss of ceramic woven fabrics. Increases in electrical conductivity result in more reflected fraction from the materials, and thus an increase in reflection loss, whereas lower electrical conductivity leads to less reflection from the material surface, and hence lower reflection loss. This relation can be explained by the increase in the electromagnetic impedance of the material as conductivity decreases. Consequently, the level of impedance mismatch to air becomes lower, reducing the reflection loss of the material. In line with this explanation, the ZE8 fabric retained the highest reflection loss following heat treatment due to its highest level of electrical conductivity (Fig. 5b).

A comparison of reflection losses of the as-received and heat-treated fabrics revealed a distinct behavior of the PN fabric. At low frequencies, reflection loss of the as-received PN fabric was about  $-5$  dB, corresponding to a  $\sim 31\%$

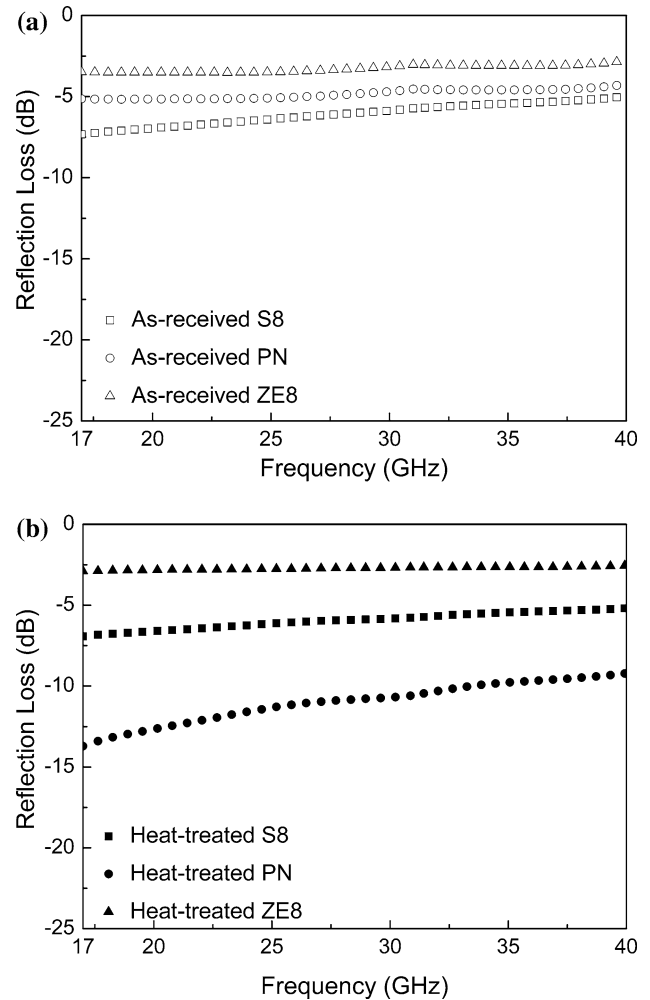


**Fig. 5** Reflection losses of single layer (a) as-received and (b) heat-treated woven fabrics

reflection of the electromagnetic wave; while at similar frequencies reflection loss of the PN-H fabric decreased to  $-14$  dB with a  $\sim 3\%$  reflection of the electromagnetic wave. The PN-type fabric is composed of carbon-coated SiC-based fibers, and the high conductivity of the carbon yielded higher reflection losses in the as-received condition. However, after heat treatment in air, as a result of the loss of the carbon coating and the formation of an oxide layer the electrical conductivity of the fiber decreased, causing a considerable difference between the reflection losses of the as-received and PN-H fabrics.

The transmission losses of the as-received and oxidized woven fabrics are plotted in Fig. 6a and b, respectively, as a function of frequency. The decreasing fraction of the transmitted wave through the material corresponds to the weakening of the transmission loss (higher negative dB). The lowest transmission losses were seen in the ZE8 fabric in both as-received and heat-treated conditions. Similar to its reflection loss, the PN fabric recorded the largest

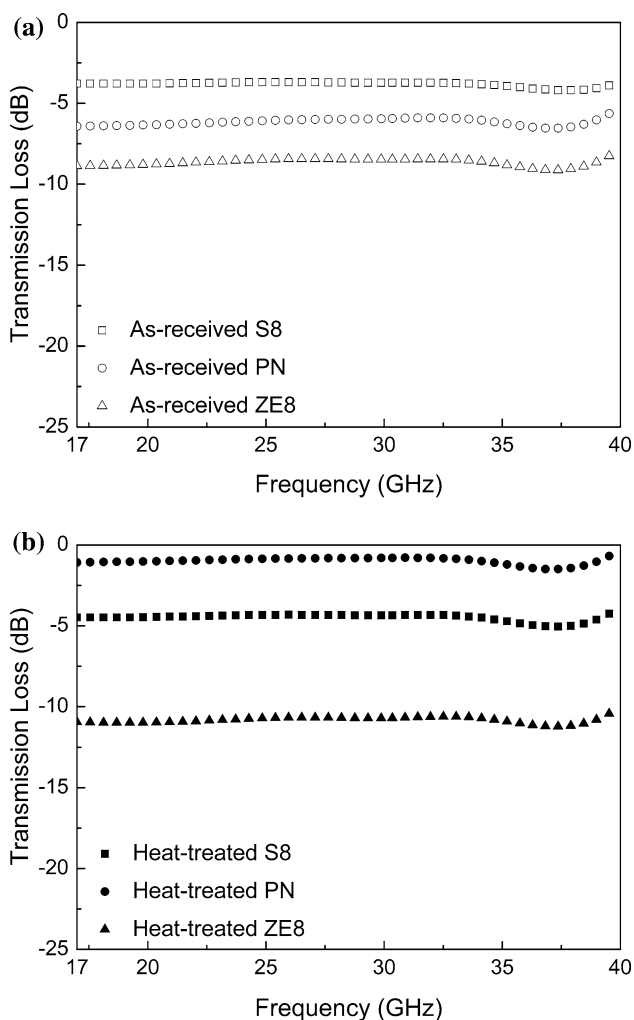


**Fig. 6** Transmission losses of single layer (a) as-received and (b) heat-treated woven fabrics

difference in transmission loss between its as-received and heat-treated states. Moreover, as a general tendency, it was observed that woven fabrics that have a higher reflectivity of electromagnetic waves also recorded lower transmission (higher reflection loss corresponds to lower transmission loss).

In line with the principle of energy conservation, incident electromagnetic radiation energy is either reflected,

transmitted, or absorbed (dissipated and converted into heat) by a material. Accordingly, the absorption percentages of the woven fabrics were calculated using Eq. 3, where %R and %T represent the reflected and transmitted portion of the electromagnetic wave, respectively. Table 3 shows the calculated absorption percentages (%) of the ceramic woven fabrics at various frequencies. The absorption percentages of single-layer SiC-based ceramic woven fabrics were <40%, which made them highly unsuitable as electromagnetic absorbing materials in commercial applications.

$$\text{Absorption percentage}(\%) = 100 - \%R - \%T. \quad (3)$$

In order to achieve a better electromagnetic wave absorption potential, several double-layer combinations of the as-received and heat-treated ceramic woven fabrics were constructed. In the first case, combinations of as-received woven fabrics were measured, among which combinations of S8 woven fabrics recorded good absorption characteristics, with both reduced reflection and transmission loss. Figure 7 shows the absorption potentials of double-layer combinations containing S8-type woven fabrics as one of the layers. A low-conductivity layer

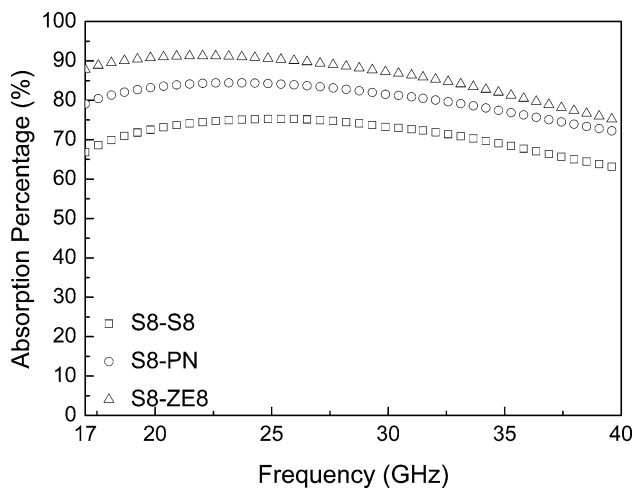


**Fig. 7** Absorption potentials of double-layer combinations with as-received S8 and other woven fabrics

**Table 3** Absorption percentages of single-layer ceramic woven fabrics

Frequency (GHz)	Absorption (%)					
	As-received S8	S8-H	As-received ZE8	ZE8-H	As-received PN	PN-H
20	37.9	42.3	42.2	39.8	46.2	15.3
25	34.3	38.4	41.0	38.6	44.3	10.6
30	31.6	37.2	37.5	37.7	40.5	8.3
35	30.5	37.6	37.5	37.4	41.2	13.3
40	25.1	28.2	30.8	34.4	32.0	10.5

(S8 woven fabric) reduced the reflection loss at the air/low-conductivity layer interface, while most of the electromagnetic wave transmitted through the woven fabric was reflected from the surface of the second layer. The low-conductivity first layer behaved as an absorbing layer, whereas the high-conductivity second layer behaved as a reflective layer, binding electromagnetic energy within the material system. In the low  $\rightarrow$  high electrical conductivity layer combinations higher absorption potentials were achieved. In this respect, the highest conductivity mismatch between the S8 and ZE8 fabrics resulted in the maximum absorption potential. Additionally, the ordering of the layers also affected the absorption potential of a given combination; for example, the absorption potential of the S8–ZE8 combination was different to that of the ZE8–S8 combination, although both combinations contained identical woven fabric layers. In the case of the S8–ZE8 combination, the electromagnetic wave was first confronted with the low-conductivity S8 woven layer, before passing through the ZE8 woven layer; whereas in the ZE8–S8 combination, the ZE8 layer was the first layer to act upon the electromagnetic wave, followed by the S8 layer. Due to the high reflection loss of the ZE8 fabric, the absorption potential was weaker in the ZE8–S8 combination.

After the investigation of the double-layer as-received woven fabrics, the absorption potentials of samples of both as-received and heat-treated layer double-layer combinations were examined. The absorption potentials of combinations of PN-H and heat-treated S8 (S8-H) fabrics with as-received ZE8 fabrics at various frequencies are compared in Table 4. It can be observed that a combination of S8-H fabrics had a slightly higher absorption potential than one of PN-H types. As there is little difference in the conductivity of heat-treated S8- and PN-type woven fabrics, the better absorption potential of the S8-type woven fabrics is believed to be a result of its smoother surface, which eliminates internal reflections.

In the final case, double-layer combinations of heat-treated fabrics were assembled. Table 5 lists the absorption potential of all combinations of heat-treated fabrics. The

**Table 4** Absorption percentages of combinations of PN-H and S8-H with ZE8-type woven fabrics

Frequency (GHz)	Absorption (%)	
	PN-H $\rightarrow$ ZE8	S8-H $\rightarrow$ ZE8
20	82.6	89.1
25	81.7	84.2
30	76.1	76.4
35	68.4	67.3
40	58.0	57.9

**Table 5** Absorption potentials of double-layer combinations with some heat-treated woven fabrics

Frequency (GHz)	Absorption (%)		
	S8-H $\rightarrow$ ZE8-H	PN-H $\rightarrow$ ZE8-H	ZE8-H $\rightarrow$ ZE8-H
20	90.7	77.4	51.7
25	90.8	83.7	49.7
30	86.2	82.8	48.5
35	80.6	79.3	48.4
40	73.5	71.5	46.5

S8-H and ZE8-H combination proved to have the best absorption potential among all samples. In the heat-treated condition, the ZE8 revealed the highest conductivity due to localized oxidation, and combinations containing the ZE8-H fabric as the second layer resulted in better absorption. A double-layer combination of ZE8-H-type woven fabrics did not improve its electromagnetic wave absorption property, as the high conductivity of the combination strengthened reflection loss.

The surface condition of the fabrics was also important in their electromagnetic wave absorption potentials. The S8 and ZE8 samples had a satin weave, and hence their surfaces were smoother than that of the plain type PN. As the smoother surface suppressed multiple reflection losses from the surface of the materials, the surface characteristics of a fabric can also be said to be important for electromagnetic wave absorption. The absorption potentials of double-layer combinations of S8 and ZE8 fabrics are shown in Fig. 8. As-received and S8-H- and ZE8-type combinations revealed similar absorption potentials, which are higher than 90% in the 18.5–26.5 GHz frequency range. This result demonstrates that heat treatment did not necessarily mean an improvement in the absorption

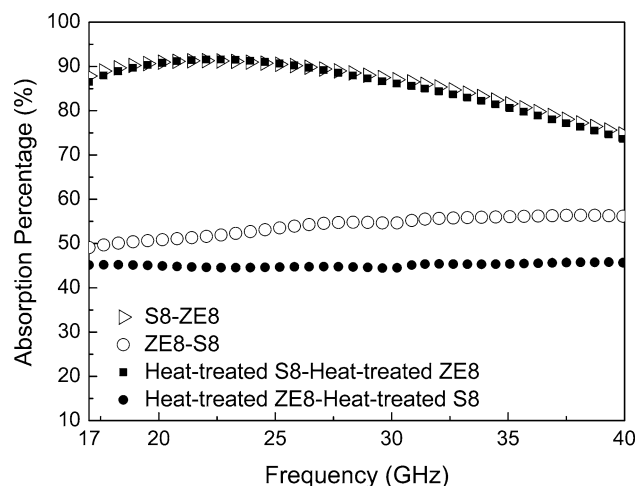


**Fig. 8** Absorption potentials of some double-layer combinations of S8- and ZE8-type woven fabrics

potential of SiC-based ceramic woven fabrics, but rather that heat treatment may be used to create woven fabrics with different electrical conductivities. In this regard, with a proper sequence of woven fabrics (low-conductivity layer before high-conductivity layer), better absorption potentials can be achieved. However, if a high electrical conductivity layer is placed in front of a low-conductivity layer, the absorption potential of the combination decreases (Fig. 8), since a significant portion of the incident electromagnetic waves were reflected from the surface before transmitting through the material. The high absorption potential of the double-layer combinations of SiC-based ceramic woven fabrics in the GHz range renders them useful as electromagnetic wave-absorbing material systems.

## Conclusion

The electromagnetic wave absorption potential of SiC-based ceramic woven fabrics was determined in the 17–40 GHz frequency range using the free-space method. The electrical conductivities of the fabrics were modified by heat treatment in air. In addition to heat treatment, the effect of different sequences of layers in combination on the electromagnetic wave absorption potential of the ceramic woven fabrics with different chemical compositions and weave types was discussed. As a result, the following conclusions have been drawn:

- Heat treatment of SiC-based woven fabrics causes a reduction in their electrical conductivity due to an oxidation of fibers. The heat-resistant ZE8 fabric was influenced least by surface modifications, whereas the carbon-coated PN-type was most affected due to the loss of its carbon-rich layer after heat treatment.
- As-received and heat-treated single-layer ceramic woven fabrics did not reveal a sufficient absorption potential (<40%) for typical applications. Various double-layer combinations of fabrics showed better electromagnetic wave absorption potentials than those of single layers.
- The sequences of layers in combinations affected the absorption potential of combinations, where low → - high electrical conductivity layer combinations led to better absorption results than other double-layer combinations.
- Combinations of heat-treated woven fabrics did not necessarily result in an improvement in absorption potential. Rather than a direct increase in absorption, the function of heat treatment was to change the electrical conductivities of the woven fabrics to achieve low → high electrical conductivity layer combinations.
- Double-layer combinations of the satin woven fabrics (S8 and ZE8) showed promising absorption characteristics compared to other combinations. S8 and ZE8 combinations in as-received and heat-treated states showed absorption potentials of higher than 90% over a wide frequency range. The high absorption potential of multi-layer SiC-based ceramic woven fabrics in the GHz range renders them as strong candidate materials for electromagnetic wave-absorbing applications.

## References

- Neelkanta PS (1995) Handbook of electromagnetic materials: monolithic and composite versions and their applications. CRC Press, Boca Raton
- Feng YB, Qiu T, Shen CY, Li XY (2006) IEEE Trans Magn 42:363
- Li J, Huang J, Qin Y, Ma F (2007) Mater Sci Eng B 138:199
- Pinho MS, Gregori ML, Nunes RCR, Soares BG (2002) Eur Polym J 38:2321
- Singh P, Babbar VK, Razdan A, Srivastava SL, Puri RK (1999) Mater Sci Eng B 67:132
- Chin WS, Lee DG (2007) Compos Struct 77:457
- Oh J-H, Oh K-S, Kim C-G, Hong C-S (2004) Composites B 35:49
- Dishovsky N, Grigorova M (2000) Mater Res Bull 35:403
- Lee CY, Song HG, Jang KS, Oh EJ, Epstein AJ, Joo J (1999) Synth Met 102:1346
- Kim T, Chung D (2006) J Mater Eng Perform 15:295
- Shui XP, Chung DDL (2000) J Mater Sci 35:1773. doi: [10.1023/A:1004784720338](https://doi.org/10.1023/A:1004784720338)
- Tellakula RA, Varadan VK, Shami TC, Mathur GN (2004) Smart Mater Struct 13:1040
- Hochet N, Berger MH, Bunsell AR (1997) J Microsc 185:243
- Kakimoto K, Shimoo T, Okamura K (1997) J Ceram Soc Jpn 105:504
- Kishimoto H, Katoh Y, Kohyama A (2002) J Nucl Mater 307:1130
- Kagawa Y, Imahashi Y, Iba H, Naganuma T, Matsumura K (2003) J Mater Sci Lett 22:159
- Kagawa Y, Matsumura K, Iba H, Imahashi Y (2007) J Mater Sci 42:1116. doi:[10.1007/10853s-006-1437-1](https://doi.org/10.1007/10853s-006-1437-1)
- Tyranno Fiber R Catalog (2001) Ube Industries Co., Ltd
- Matsumura K, Kagawa Y (2007) J Mater Sci 42:3251. doi: [10.1007/s10853-006-1413-9](https://doi.org/10.1007/s10853-006-1413-9)
- Seo IS, Chin WS, Lee DG (2004) Compos Struct 66:533
- Ghodgaonkar DK, Varadan VV, Varadan VK (1990) IEEE Trans Instrum Meas 39:387
- Shimoo T, Morisada Y, Okamura K (2002) J Mater Sci 37:4361. doi:[10.1023/A:1020608704120](https://doi.org/10.1023/A:1020608704120)
- Duffrene L, Kieffer J (1998) J Phys Chem Solid 59:1025